DOI: 10.18721/JPM.12111
УДК 519.63

A POSTERIORI ERROR ESTIMATE FOR REISSNER–MINDLIN PLATES: VERIFICATION OF IMPLEMENTATIONS AND NUMERICAL TESTING

K.V. Kiselev[1], *M.E. Frolov*[1], *O.I. Chistiakova*[1]

[1]Peter the Great St. Petersburg Polytechnic University, St. Petersburg, Russian Federation

A posteriori error estimate for accuracy control of approximate solutions for the problem of Reissner–Mindlin plates bending has been analyzed in the paper. The estimate was constructed using the functional approach based on rigorous mathematical grounds, in particular, on methods of functional analysis. It is valid for all conforming approximations of exact solutions, and therefore, it is robust. The estimate is guaranteed in practical implementations due to reliability of the respective inequality. The above-mentioned properties of the method of error control are very desirable for engineering analysis, where some details of computations might be hidden. Our paper investigated two independent implementations of the estimate. Using specially constructed numerical tests, correctness of both implementation algorithms and similarity of the obtained results for all examples were shown. An overestimation of the true error was established to remain acceptable for a wide range of plate thickness values.

Keywords: a posteriori error estimate, finite element method, Reissner – Mindlin plate

Citation: K.V. Kiselev, M.E. Frolov, O.I. Chistiakova, A posteriori error estimate for Reissner – Mindlin plates: verification of implementations and numerical testing, St. Petersburg State Polytechnical University Journal. Physics and Mathematics. 12 (1) (2019) 117–129. DOI: 10.18721/JPM.12111

ВЫЧИСЛИТЕЛЬНЫЙ ЭКСПЕРИМЕНТ И ВЕРИФИКАЦИЯ РЕАЛИЗАЦИЙ АПОСТЕРИОРНОЙ ОЦЕНКИ ДЛЯ ПЛАСТИН РЕЙССНЕРА – МИНДЛИНА

К.В. Киселев[1], *М.Е. Фролов*[1], *О.И. Чистякова*[1]

[1]Санкт-Петербургский политехнический университет Петра Великого, Санкт-Петербург, Российская Федерация

В работе рассматривается апостериорная оценка точности приближенных решений задачи об изгибе пластин Рейсснера – Миндлина. Оценка построена при помощи функционального подхода, основанного на строгих математических методах, в частности методах функционального анализа. Она справедлива для любых конформных аппроксимаций точных решений, что делает ее надежной. Она также является гарантированной, и неравенство не нарушается при практической реализации. Эти свойства делают данный метод контроля точности решений привлекательным для использования в инженерных расчетах, где некоторые вычислительные детали могут быть скрыты. В статье исследованы две независимые реализации оценки. Использование вычислительного эксперимента показало корректность работы алгоритмов и близость полученных результатов. Установлено, что для широкого диапазона значений толщины степень переоценки истинной величины погрешности остается приемлемой.

Ключевые слова: апостериорная оценка погрешности, метод конечных элементов, пластина Рейсснера – Миндлина

Ссылка при цитировании: Киселев К.В., Фролов М.Е., Чистякова О.И. Вычислительный эксперимент и верификация реализаций апостериорной оценки для пластин Рейсснера – Миндлина // Научно-технические ведомости СПбГПУ. Физико-математические науки. 2019. Т. 12. № 1. С. 128–141. DOI: 10.18721/JPM.12111

Introduction

The study is dedicated to a posteriori control of exact solutions in problems of plate theory, often considered in different engineering computations. Whether the results of the computation are close to the experiment depends on how adequately the selected model describes the real physical processes occurring during deformation of the given object.

In this paper, we have investigated the problem of controlling the accuracy of the finite element method (FEM) for a model of linearly elastic deformable Reissner–Mindlin plates [1]. This model is typically used for plates of small and medium thickness. Unlike the classical Kirchhoff–Love model which describes plates with a small ratio of thickness to characteristic size, the Reissner–Mindlin model makes it possible to consider plates of medium thickness by abandoning the assumption that fibers normal to the midplane of the plates preserve this property upon application of loads.

The system of equilibrium equations for the Reissner–Mindlin model has the following form:

$$\begin{cases} -\mathrm{Div}(C\varepsilon(\theta)) = \gamma, \\ -\mathrm{div}\gamma = g, \\ \gamma := \lambda t^2(\nabla u - \theta), \end{cases} \quad \text{in the region } \Omega, \quad (1)$$

where u is the scalar deflection field of the midplane, θ is the vector field of rotations of the normal to the midplane; γ is the vector field corresponding to the pair (u, θ); ε is the strain tensor; t is the plate thickness; gt^3 is the distributed transverse load; C is a fourth-order symmetric tensor; Ω is the plane region occupied by the plate;

$$\lambda = \frac{1}{2} Ek / (1+\nu)$$

(E is Young's modulus, ν is Poisson's ratio, k is the correction coefficient; $k = 5/6$ is taken in many computations).

There are several well-known commercial packages for performing computations within the framework of this model using FEM. Since products of this type, such as ANSYS (a computing package popular among engineers), are closed-source, it proves impossible to understand in full detail how the necessary computations were performed. As a result, it might be difficult to estimate the magnitude of the error if either the corresponding rigorous mathematical model has not been developed or the error estimate obtained using this model has not been formulated. Substantial deviations from experimental data may also be due to such factors as incorrectly chosen model, errors in applying it, and poor quality of computations with a fairly adequate model.

Thus, an important task is to construct and numerically study an a posteriori estimate for the accuracy of an approximate solution that is guaranteed and robust, i.e., would not allow for underestimation of the error in practical implementation and would not depend on hidden details of the computation procedure.

The first version of such estimate was obtained in [2] based on the functional approach and modified in [3]. The recent results concerning its numerical implementation were reviewed in [4]. The evolution of the functional approach from 1996 to the present can be traced from the sources cited in monographs [5–7] and recently published papers [8, 9]. Reviews of other approaches applied to the given problem can be found, for example, in [10, 11] and the citations therein.

Such a posteriori assessments have the following general form:

$$\| u - \tilde{u} \| \leq \leq M(\tilde{u}, D, \tilde{\tilde{y}}_1, \tilde{\tilde{y}}_2, ..., c_1, c_2, ...), \quad (2)$$

where the norm of deviation of the unknown exact solution u from the obtained approximate solution $\tilde{u}$ is considered on the left-hand side; it is selected based on the problem statement; the functional M that is the deviation majorant is on the right-hand side. The approximate solution $\tilde{u}$, the parameters of the problem D and the set of constants $(c_1, c_2, ...)$ are arguments of the functional. Importantly, the values of these constants depend on the properties of the problem but not on the properties of the partition. Finally, $(\tilde{\tilde{y}}_1, \tilde{\tilde{y}}_2, ...)$ is a set of free elements.

The functional M should satisfy a natural condition that it should give a zero value if and only if the approximate solution coincides with the exact solution.

At the same time, it seems no less important and useful to know not only the magnitude of the global error of the approximate solution but also of the local distribution of the error over the partition elements. This allows to select the regions with the greatest deviation of the approximate solution from the exact one. Next, instead of refining the entire mesh, the necessary improvements are introduced only for elements with large error. This approach is called adaptive; it helps reduce the computational resources it takes to obtain a solution of the desired quality.

Thus, the full cycle of computations using the adaptive approach takes the following form:

initial partition of region →
obtain solution →
estimate global error
(exit from computation cycle
when required accuracy
is reached) →
find regions (3)
with the greatest local
errors → refine mesh
in selected regions →
computation on new mesh →
obtain more accurate solution

This cycle can be applied to solving real engineering problems provided that the properties of the given estimate can be confidently predicted and a set of parameters for which robust results are obtained can be determined.

We have previously obtained (first Frolov, and then Chistiakova, see the review in [4]) two independent implementations of the a posteriori estimate for Reissner–Mindlin plates: in the FORTRAN language and in the MATLAB package. We have conducted an initial study assessing the robustness of the results for each of the algorithms giving a numerical value of the estimate. It is now seems necessary to expand the study of behavior of a posteriori estimates by examining more examples in order to assess whether the correctness of the given tool, the robustness of the results, and lay the foundations for further improving the method.

The goal of this study has consisted in comparative analysis of two implementations for computing the a posteriori estimate of the accuracy of an approximate solution to the Reissner–Mindlin plate bending problem. Analysis includes constructing examples with different specifics, computing different thicknesses and comparing the estimated values as well as the accompanying auxiliary parameters.

Mathematical statement of the problem

Let us consider the system of equations describing the Reissner–Mindlin model for linearly elastic plates of thickness t. The problem is formulated in terms of a scalar function $u = u(x)$ describing the deflection of the midplane at the point x and a vector function $\theta = \theta(x)$ describing the angles of rotation of the normal to the midplane. The midplane initially occupies a bounded simply-connected region $\Omega \subset \mathbb{R}^2$ with a Lipschitz-continuous boundary Γ.

Problem statement: *Find the pair* (u,θ) *and the vector field* $\gamma = \gamma(x)$ *corresponding to this pair, which would satisfy system of equations* (*1*).

The solution is sought in a generalized sense. We assume that $g \in \mathbb{L}_2$, the tensor C is symmetric, there is a pair of constants ξ_1 and ξ_2 such that a two-way estimate holds true:

$$\xi_1 |\kappa|^2 \le C\kappa : \kappa \le \xi_2 |\kappa|^2$$

$\forall \kappa \in \mathbb{M}^{2\times 2}_{\text{sym}}$, $|\kappa|^2 = \kappa : \kappa$, where $\mathbb{M}^{2\times 2}_{\text{sym}}$ is a space of symmetric tensors of rank 2 and dimension 2.

While this study examines plates made of homogeneous isotropic material, this is not a fundamental limitation.

Let us consider the boundary Γ of the dos main Ω, and represent it as two components: Γ_D, $\Gamma_D \neq \varnothing$, where the plate is clamped, i.e., the conditions for the displacement $u = 0$ and rotation $\theta = 0$ are given, and $\Gamma_S = \Gamma \backslash \Gamma_D$, where the plate has free boundary conditions (other types of boundary conditions can be considered as well).

Generalized statement of the problem on Reissner–Mindlin plate bending: *find such a set of three elements* $(u,\theta,\gamma) \in U \times \Theta \times Q$, *where*

$$\begin{cases} U = \left\{\omega \in \mathbb{W}_2^1(\Omega) \mid \omega = 0 \text{ on } \Gamma_D\right\}, \\ \Theta = \left\{\varphi \in \mathbb{W}_2^1(\Omega) \times \mathbb{W}_2^1(\Omega) \mid \varphi = 0 \text{ on } \Gamma_D\right\}, \\ Q = \mathbb{L}_2(\Omega) \times \mathbb{L}_2(\Omega), \end{cases}$$

which satisfies the relations

$$\begin{cases} \int\limits_\Omega C\varepsilon(\theta) : \varepsilon(\varphi) d\Omega - \\ -\int\limits_\Omega \gamma \cdot \varphi \, d\Omega = 0, \ \forall \varphi \in \Theta; \\ \int\limits_\Omega \gamma \cdot \nabla\omega \, d\Omega = \\ = \int\limits_\Omega g\omega \, d\Omega, \ \forall \omega \in U; \\ \int\limits_\Omega (\lambda^{-1} t^2 \gamma - (\nabla u - \theta)) \cdot \tau \, d\Omega = 0, \\ \forall \tau \in Q. \end{cases} \quad (4)$$

The energy functional in the problem has the following form:

$$J(u,\theta) = \int\limits_\Omega \left(\frac{1}{2} C\varepsilon(\theta) : \varepsilon(\theta) + \right. \\ \left. + \frac{1}{2} \lambda t^{-2} |\nabla u - \theta|^2 - gu \right) d\Omega. \quad (5)$$

The corresponding minimization problem is set in the space

$$S := U \times \Theta.$$

Let us proceed directly to the type of the given a posteriori estimate. Let there be a pair of conformal approximations $(\tilde{u}, \tilde{\theta})$ of the exact solution of the problem (u,θ) in S, then the vector field

$$\gamma = \lambda t^{-2}(\nabla u - \theta)$$

is approximated in space Q by the element

$$\tilde{\gamma} = \lambda t^{-2}(\nabla \tilde{u} - \tilde{\theta}).$$

Let us introduce three deviations for each of the solution components:

$$e_{\tilde{u}} = u - \tilde{u},$$
$$e_{\tilde{\theta}} = \theta - \tilde{\theta},$$
$$e_{\tilde{\gamma}} = \gamma - \tilde{\gamma}.$$

Let us then introduce the squared error, expressed in terms of the difference between the values of the energy functional:

$$\tilde{\varepsilon}^2 = J(\tilde{u}, \tilde{\theta}) - J(u, \theta).$$

It was proved (see [2]) that for $\forall(\tilde{u}, \tilde{\theta}) \in S$, there is a ratio

$$\tilde{\varepsilon}^2 = \frac{1}{2}\left(||| e_{\tilde{\theta}} |||^2 + \lambda^{-1} t^2 \| e_{\tilde{\gamma}} \|_\Omega^2 \right),$$

where

$$||| e_{\tilde{\theta}} |||^2 := \int_\Omega C\varepsilon(e_{\tilde{\theta}}) : \varepsilon(e_{\tilde{\theta}})\, d\Omega,$$

$$\| e_{\tilde{\gamma}} \|_\Omega^2 := \int_\Omega | e_{\tilde{\gamma}} |^2 d\Omega.$$

Next, we introduce the free elements necessary for constructing the a posteriori estimate: the vector field $\tilde{\tilde{y}}$ and the asymmetric tensor $\tilde{\tilde{\kappa}}$ represented as its components $\tilde{\tilde{\kappa}} = [\tilde{\tilde{\kappa}}^1, \tilde{\tilde{\kappa}}^2]$. They are selected such that

$$\tilde{\tilde{y}}, \tilde{\tilde{\kappa}}^1, \tilde{\tilde{\kappa}}^2 \in \mathbb{H}(\Omega, \mathrm{div}) :=$$
$$:= \{ y \in \mathbb{L}_2(\Omega)\, \mathbb{L}_2(\Omega) \mid \mathrm{div} y \in \mathbb{L}_2(\Omega) \}.$$

Upon applying identity transformations and known inequalities (given in [3]), the final inequality takes the form:

$$||| e_{\tilde{\theta}} |||^2 + \lambda^{-1} t^2 \| e_{\tilde{\gamma}} \|_\Omega^2 \le \hat{a}^2 + \lambda^{-1} t^2 \hat{b}^2, \qquad (6)$$

where

$$\hat{a} = ||| C^{-1}\mathrm{sym}(\tilde{\tilde{\kappa}}) - \varepsilon(\tilde{\theta}) ||| +$$
$$+ c_1 \| \mathrm{skew}(\tilde{\tilde{\kappa}}) \|_\Omega + c_2 c_3 (|\Omega| \| g + \mathrm{div}\tilde{\tilde{y}} \|_\Omega^2 +$$
$$+ |\Gamma_S| \| \tilde{\tilde{y}} \cdot n \|_{\Gamma_S}^2)^{1/2} +$$
$$+ c_4 (|\Omega| \| \tilde{\tilde{y}} + [\mathrm{div}\tilde{\tilde{\kappa}}^1, \mathrm{div}\tilde{\tilde{\kappa}}^2] \|_\Omega^2 +$$
$$+ |\Gamma_S| \| [\tilde{\tilde{\kappa}}^1 \cdot n, \tilde{\tilde{\kappa}}^2 \cdot n] \|_{\Gamma_S}^2)^{1/2}, \qquad (7)$$
$$\hat{b} = \| \tilde{\tilde{y}} - \tilde{\gamma} \|_\Omega +$$
$$+ c_3 (|\Omega| \| g + div\tilde{\tilde{y}} \|_\Omega^2 +$$
$$+ |\Gamma_S| \| \tilde{\tilde{y}} \cdot n \|_{\Gamma_S}^2)^{1/2},$$
$$c_1, c_2, c_3, c_4 \in \mathbb{R}.$$

The constants in the last row depend only on the geometry of the domain Ω, the boundary conditions and the properties of the material, and are a consequence of the following inequalities:

$$\| \nabla\varphi \|_\Omega^2 \le c_1^2 ||| \varphi |||^2,$$

$$\| \varphi \|_\Omega^2 \le c_2^2 ||| \varphi |||^2,$$

$$\frac{1}{|\Omega|} \| \omega \|_\Omega^2 + \frac{1}{|\Gamma_S|} \| \omega \|_{\Gamma_S}^2 \le$$
$$\le c_3^2 \| \nabla\omega \|_\Omega^2,$$

$$\frac{1}{|\Omega|} \| \varphi \|_\Omega^2 + \frac{1}{|\Gamma_S|} \| \varphi \|_{\Gamma_S}^2 \le$$
$$\le c_4^2 ||| \varphi |||^2.$$

Procedure for implementing the computational experiment

Let us consider in detail the steps of adaptive algorithm (3), which is typically used to refine the approximate solution more effectively.

The geometry of the given region, the thickness of the plate and the parameters of the material are set and initial partition is constructed as a first step. Next, the computations are performed in a suitable package, for example, ANSYS.

Once the values of displacements and rotations in the mesh nodes have been obtained, the algorithm moves on to the next step, which involves applying the given a posteriori estimate and finding the global error value. It is defined for the entire solution as the root of the sum of squared local errors for each element, called indicators. If the global error value is unsatisfactory within the framework of the problem set, the distribution of indicators over the partition elements is considered.

If the distribution of local errors has been obtained, it becomes possible to select the regions with the highest error value. There are several strategies for selecting elements (see, for example, [12, 13]); they consist in finding the threshold value of the indicator for which selecting too many or too few elements is not allowed globally.

The final part of each cycle of the adaptive algorithm is refining the mesh (and coarsening it in the general case) in the selected regions. The task is neither trivial nor auxiliary because the quality of the mesh affects the accuracy of the computations. The conformality of the mesh has to be preserved; the mesh angles should lie within a certain range, as too small and too large angles negatively affect the accuracy of the computations; in case of symmetry, it is also highly desirable to preserve its character. Different algorithms that solve this problem for quadrilateral elements are considered, in particular, in [14].

Next, the problem is recomputed for a new partition. This adaptive iterative algorithm implies that the result obtained on a modified mesh can again be assessed for accuracy and distribution of error over the computational domain.

Numerical results and discussion

The comparative analysis in this study was carried out for four computational examples with different specifics: a circular plate, a skew plate, a square plate with a large square hole, a square plate with a small circular hole.

Each of these cases has its own specifics which can be indicators of imperfections in the implementations. For example, a square plate with a large square hole has stress concentration zones near the top of hole. The analytical solution is known for the circular plate. A uniformly distributed load is considered in all examples. Oblique plates are also discussed in studies on a posteriori estimates [15, 4]; we used this type of plate in our study to illustrate the behavior of the error with rigidly clamped boundary conditions only imposed on the upper and lower edges (the two other edges remain free), in contrast to the other examples, considering fully clamped edges.

Let us now describe two examples. Notably, while we had to omit some of the results obtained for brevity's sake, they fully confirm the conclusions we ultimately reached.

We generated the region's geometry, imposed boundary conditions, constructed the mesh and obtained the actual solution using the ANSYS Mechanical (APDL) package. The MATLAB solver was also used for verification.

The effectiveness index I_{eff} is introduced to analyze the effectiveness of the estimate; this characteristic is commonly used in theory of a posteriori accuracy control, defined as the ratio of the majorant to the norm of deviation of the approximate solution from the exact one,

$$I_{eff} = M / \| u - \tilde{u} \|.$$

Thus, I_{eff} indicates the degree of error overestimation. Accordingly, the closer its value approaches unity from the right, the better. If the analytical solution of the problem is unknown, the approximate solution computed on a very fine mesh is taken as the exact solution u. This technique always yields slightly overestimated values of I_{eff}, and the actual estimation produces even better results than what we can verify.

The implementations are compared by the most important parameters. First, the constants c_1, c_2, c_3 and c_4 are considered. To compute c_1, we additionally consider a constant c_k in the Korn inequality. The important role of this constant in a posteriori estimates for problems of elasticity theory of elasticity is discussed, in particular, in monograph [6]. Then,

$$c_1 = c_k \sqrt{12(1+\nu)} / E$$

(for problems where $\Gamma_s = \emptyset$, $c_k = \sqrt{2}$).

Next, we compare the error e that is the square root of the left-hand side of estimate (6); the majorant M that is the square root of the right-hand side of estimate (6) and its components D, S, R, where

$$D = \| C^{-1}\mathrm{sym}(\tilde{\kappa}) - \varepsilon(\tilde{\theta}) \| + \\ + \lambda^{-1/2} t \, \| \tilde{\tilde{y}} - \tilde{\gamma} \|_{\Omega},$$

$$S = c_1 \, \| \mathrm{skew}(\tilde{\kappa}) \|_{\Omega},$$

$$R = c_2 c_3 \Big(|\Omega| \, \| g + \mathrm{div}\tilde{\tilde{y}} \|_{\Omega}^2 + \\ + |\Gamma_S| \, \| \tilde{\tilde{y}} \cdot n \|_{\Gamma_s}^2 \Big)^{1/2} + \\ + \lambda^{-1/2} t \, c_3 \Big(|\Omega| \, \| g + \mathrm{div}\tilde{\tilde{y}} \|_{\Omega}^2 + \\ + |\Gamma_S| \, \| \tilde{\tilde{y}} \cdot n \|_{\Gamma_s}^2 \Big)^{1/2} + \\ + c_4 \Big(|\Omega| \, \| \tilde{\tilde{y}} + [\mathrm{div}\tilde{\tilde{\kappa}}^1, \mathrm{div}\tilde{\tilde{\kappa}}^2] \|_{\Omega}^2 + \\ + |\Gamma_S| \, \| [\tilde{\tilde{\kappa}}^1 \cdot n, \tilde{\tilde{\kappa}}^2 \cdot n] \|_{\Gamma_s}^2 \Big)^{1/2};$$

the last of the compared quantities is the efficiency index I_{eff}.

The degree of refinement of the mesh is denoted as R_i, $i \in \{0, 1, 2, 3, 4, 5\}$, where the zero index corresponds to the initial partition.

To compute the majorant M, constants (7) are first approximately computed once for each example, and the results can then be used to obtain the error distribution on all meshes and thicknesses. The computation of the constants is asymptotic with respect to refinement of the mesh R_i; satisfactory values are obtained even on relatively coarse meshes, which is important for potential practical applications of the method.

The auxiliary second block includes searching for a reference solution on fine meshes and computing the energy functional value based on this solution. This is only done for the purpose of the computational experiment and is not required in real engineering problems, where it is simply replaced by computing the functional a posteriori estimate on the current mesh (this task is far less resource-consuming in terms of computational costs).

The final third block is responsible for directly computing the majorant M, where certain c_1, c_2, c_3, c_4, which are somewhat overestimated to provide robustness, are fed to the input.

Let us consider the comparison results, obtained using the examples of the circular plate and the square plate with a large square hole.

Example 1. Round plate. Let us start with a classic example (see ANSYS Verification Manual), where the analytical value of the deflection in the center of the plate is known.

Fig. 1 shows the deformations of the circular plate of average thickness t, computed in ANSYS on an R_1 mesh. The parameters of the model are given in Table 1.Table 2 contains the values of the computed auxiliary constants and allows to compare the performance of both implementations on different meshes. As mentioned above, mesh convergence of the constant values is observed with decreasing sizes of mesh elements. Due to zero boundary conditions, the exact value of the constant c_k is known and equals $\sqrt{2}$. For further computations, the constants obtained on the R_2 mesh are used, overestimated to provide robustness (see column R_2^*).

Table 3 contains the main computed results for comparison, namely the majorant M and its components. Let us consider the upper section of the table, i.e., the case where $Rad/t = 250$. Evidently, the

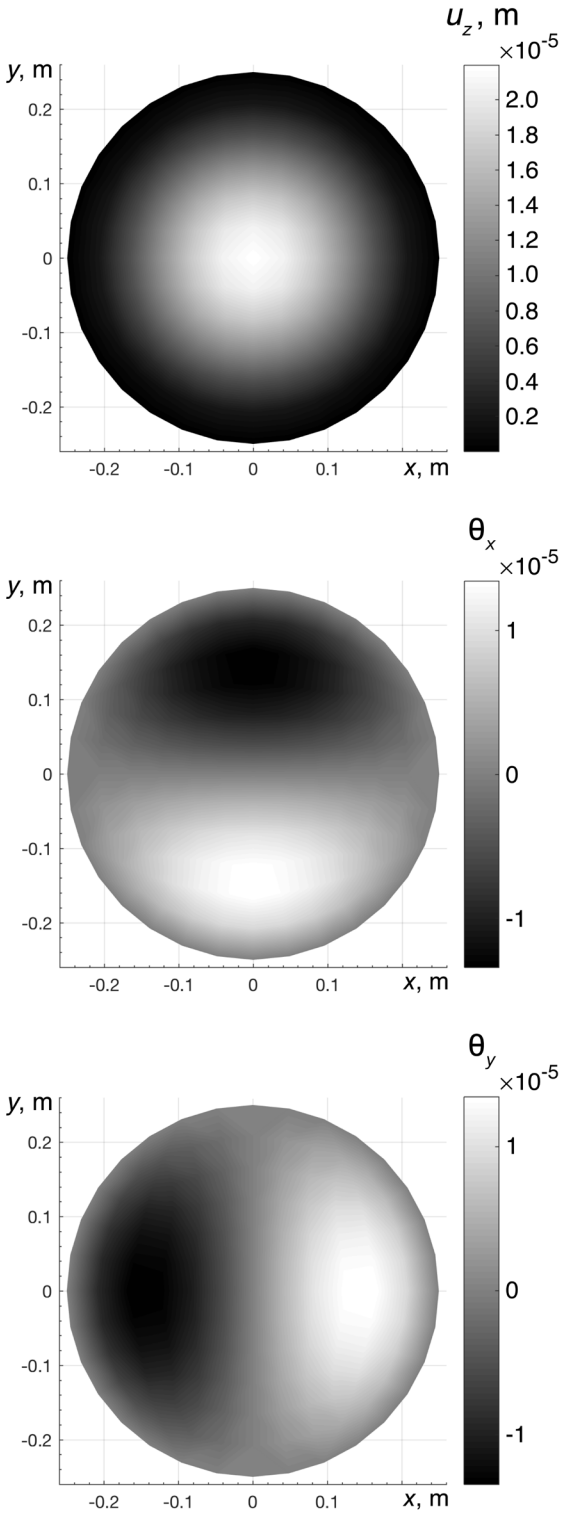

Fig. 1. Computed deformation of circular plate with average thickness in ANSYS on R_1 mesh; u_z is the distribution of the deflection of the midplane; θx, θy are the distributions of the fields of rotation of the normal to the midplane. $Rad/t = 250$ (see the data in Table 1)

Table 1

Model of circular plate

Parameter	Value	Specifics
Young's modulus E, N/m2	2·1011	1. The edge of the plate is fully clamped 2. The mesh constructed in the region has a structure of the general form
Poisson's ratio ν	0.3	
Load, N/m2	6585.175	
Radius Rad, m	0.25	
Thickness t, m	10^{-3}; $5 \cdot 10^{-5}$	

Table 2

Constants for circular plate computed in FORTRAN and MATLAB implementations

Mesh	Number of elements	Constant value				
		c_k	c_1	c_2	c_3	c_4
R_0	32	1.39 1.42	1.23e − 05 1.25e − 05	9.15e − 07 9.01e − 07	0.23	2.09e − 06 2.06e − 06
R_1	128	1.41 1.42	1.25e − 05	9.36e − 07 9.32e − 07		2.12e − 06 2.11e − 06
R_2	512	1.42		9,42e − 07 9.41e − 07		2.13e − 06
R_2^*	512	–	1.30e − 05	9.50e − 07	0.30	2.20e − 06

Notes. 1. The upper numbers in the cells of the table refer to the FORTRAN implementation, the lower to MATLAB; *a single number is given when the data coincide here and below*. 2. The data for the mesh marked with an asterisk correspond to the upper bound, overestimated for reliability. 3. $Rad/t = 250$.

Table 3

Control values of inequality (6) for circular plates of medium and small thickness in two implementations on R_2 mesh

Component of majorant (and majorant)	Control value	
	FORTRAN	MATLAB
$Rad/t = 250$		
e	0.712e + 02	
M	0.114e + 03	
D	0.111e + 03	
S	0.271e + 01	0.272e + 01
R	0.723e + 00	
I_{eff}	1.60	
$Rad/t = 5000$		
e	0.114e + 12	
M	0.162e + 12	
D	0.162e + 12	
S	0.217e + 08	
R	0.568e + 07	
I_{eff}	1.42	

term D plays the determining role, since this component includes the parts of the estimate corresponding to the error terms. The components S and R should be close to zero in the fields close to exact, which is what is observed. The values of I_{eff} given in rows 6 and 12 of the table allow to estimate the degree of overestimation for both implementations. It can be seen that the values computed by the two algorithms (I_{eff} = 1.60 in row 6) coincided, and the value itself is satisfactory, that is, there is no critical overestimation (by an order of magnitude or by several times).

Fig. 2 illustrates the distribution of local error indicators in a region of the circular plate on an R_2 mesh. The indicators are identical and suggest that the error is distributed not only in the zone of maximum plate deflection, but also near the region's

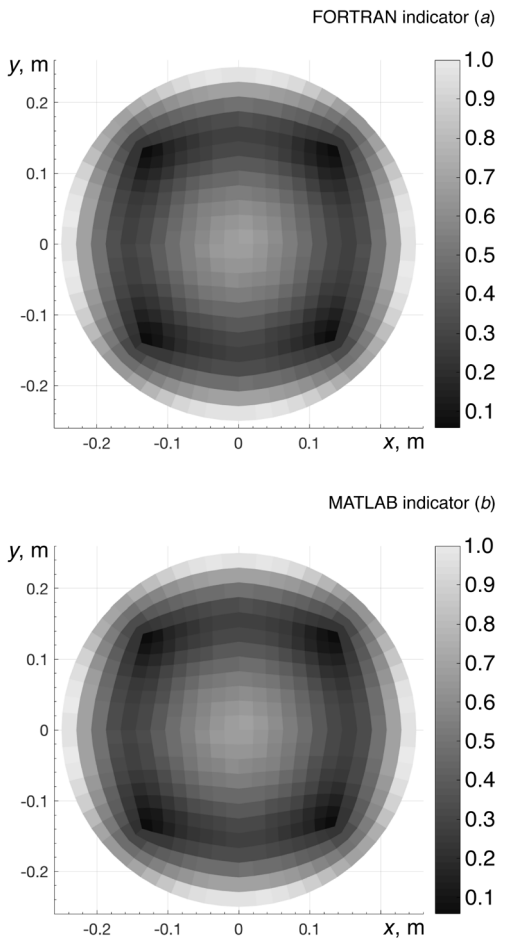

Fig. 2. Computed distributions of local error indicator over elements of region of circular plate in FORTRAN (*a*) and MATLAB (*b*) implementations on R_2 mesh; Rad/t = 250 (see Example 1)

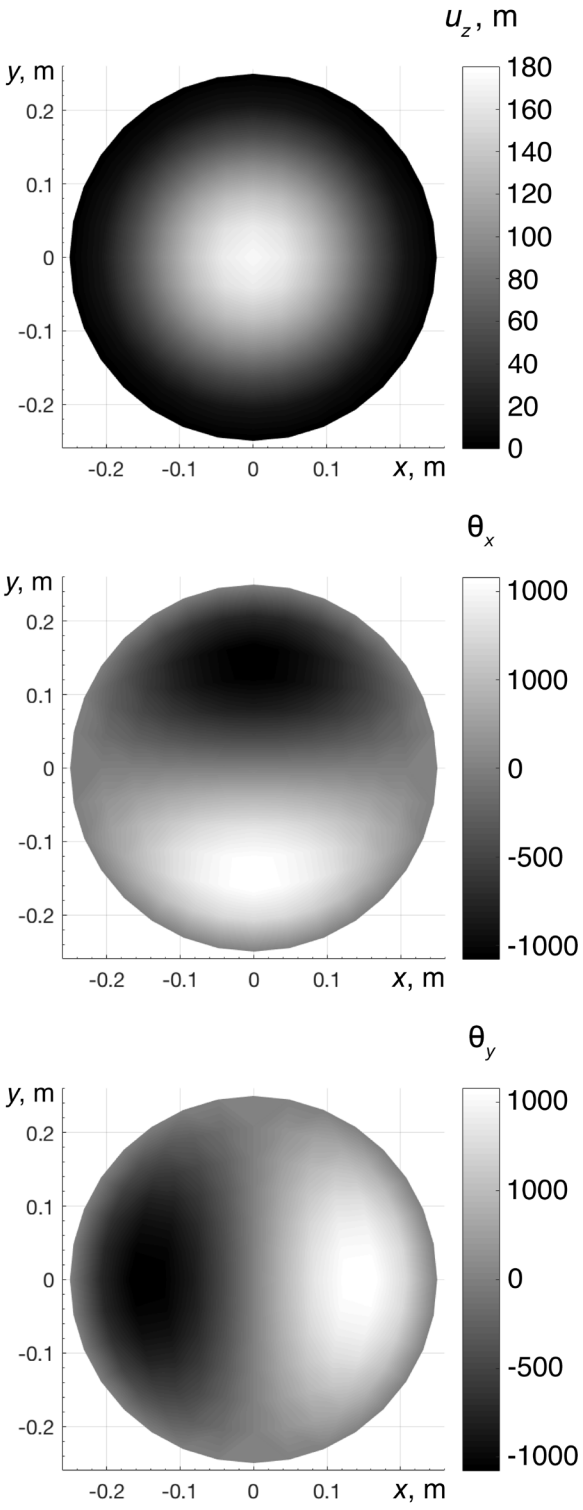

Fig. 3. Computed results similar to Fig. 1 for circular plate with small thickness; Rad/t = 5000 (see Table 1)

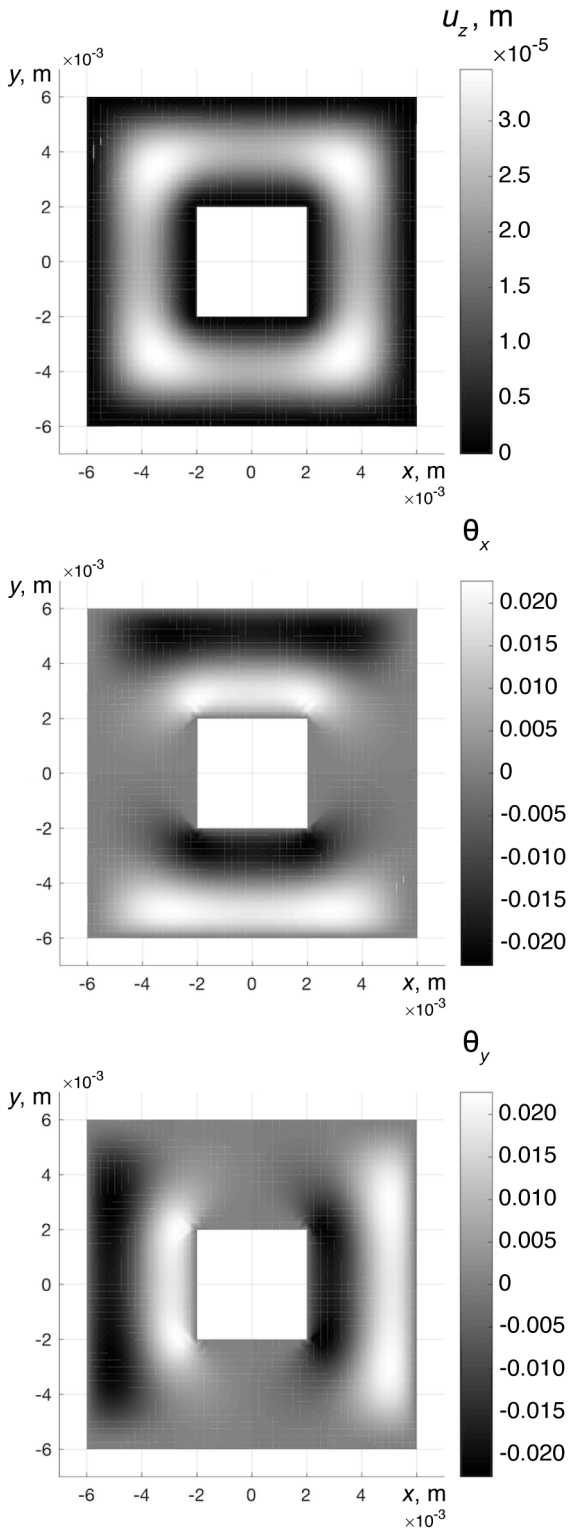

Fig. 4. Computed deformation of square plate with large square hole;
ANSYS was used on R_1 mesh.
Notations for the quantities are the same as in Fig. 1

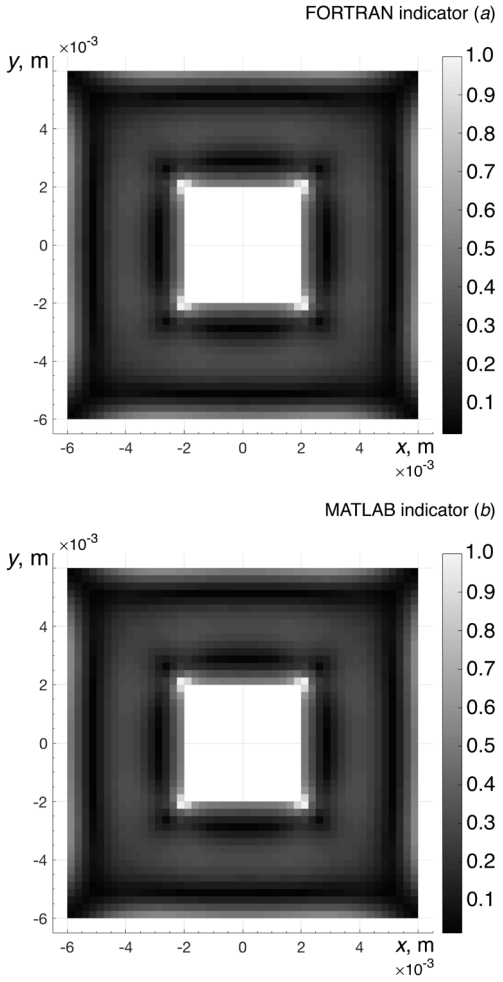

Fig. 5. Computed distributions of local error indicator over elements of region in FORTRAN (*a*) and MATLAB (*b*) implementations on R_2 mesh;
$A/t = 120$ (see Example 2)

boundary. This corresponds to the structure of the energy norm in this problem (this norm is defined in terms of gradients, which are computed with less accuracy at the edge). The lack of complete symmetry is due to the specifics of mesh construction.

Next, let us consider the computed results for a thin round plate with a thickness $t = 0.00005$ m ($Rad/t = 5000$), where the material parameters and the type of boundary conditions remained the same (see Table 1). This allows to assess the effectiveness of the method depending on plate thickness which is the key parameter in this case.

Fig. 3 shows an approximate solution. Evidently, the maximum value of the midplane deflection increased, compared with that in Fig.1. Changing the plate

Table 4

Model of square plate with large square hole

Parameter	Value	Specifics
Young's modulus E, N/m^2	$2 \cdot 10^9$	1. The plate's outer and inner edges are fully clamped 2. Mesh elements are square 3. The solution has stress concentration zones
Poisson's ratio ν	0.3	
Load, N/m^2	6585.175	
Side of square, m outer A inner a	 $12 \cdot 10^{-3}$ $4 \cdot 10^{-3}$	
Thickness t, m	10^{-4}	

Table 5

Computed constants in two implementations for square plate with large square hole

Mesh	Number of elements	Implementation	Constant value				
			c_k	c_1	c_2	c_3	c_4
R_1	512	FORTRAN	1.41	1.25e − 04	1.46e − 07	0.12	1.29e − 05
		MATLAB	1.42				1.28e − 05
R_1^*			−	1.30e − 04	1.50e − 07	0.15	1.30e − 05

Notes. 1. Data for the mesh marked with an asterisk correspond to the upper bound, overestimated for reliability. 2. The geometrical parameter $A/t = 120$.

Table 6

Control values of inequality (6) in two implementations on R_2 mesh for squareplate with large square hole

Component of majorant (and majorant)	Control value	
	FORTRAN	MATLAB
e	0.313e + 04	
M	0.529e + 04	0.534e + 04
D	0.519e + 04	0.515e + 04
S	0.413e + 02	0.348e + 02
R	0.567e + 02	0.161e + 03
I_{eff}	1.69	1.70

thickness does not affect the geometry of the region, and, therefore, the computed values of constants (7). Comparing the values in rows 6 and 12 of Table 3, we can also conclude that the value of the I_{eff} index decreased from 1.60 to 1.42 for a thin plate, i.e., it was close to unity that is the optimal value.

The computed distributions of local error indicators over a region of a circular plate with small thickness t = 0.00005 m (Rad/t = 5000) on an R_2 mesh have the form close to that shown in Fig. 2, so they are not given in this paper. Based on the obtained data, we can conclude that the algorithms work correctly for a fairly wide range of thicknesses, which is confirmed by other studies.

Example 2. Square plate with a large square hole. The following example was considered in order to explore the behavior of the estimate in stress concentration zones. Naturally, similar regions form near the tops of the inner hole with this plate configuration.

Fig. 4 shows the computed deformations of a square plate with a large square hole. The computations were performed in ANSYS on an R_1 mesh. The distributions of the quantities u_z, θ_x and θ_y over a region of the plate are given. As in Example 1, u_z is the midplane deflection; θ_x, θ_y are the distributions of the rotation fields.

Table 5 contains the computed auxiliary constants. For further computations, we used the overestimated values of the constants obtained on the R_1 mesh (data in row R_1^*).

Let us consider the results of the comparison of reference values of the estimate on the R_2 mesh. It can be seen from the data in Table 6 that the values of I_{eff} for the two implementations practically coincide, and no considerable overestimation is observed.

Let us consider the data shown in Fig. 5. The results of the implementations coincide, the distributions of the indicator are almost identical. The zones with the minimum error are located in the corners of the outer edge. Due to boundary conditions, the nodes have minimal displacement in these points. The zones with the maximum error are located in the regions where the stresses exhibit singularities if loads are applied.

Conclusion

In this study, we have compared the results obtained using existing implementations of the algorithms for computing the functional a posteriori estimate for Reissner–Mindlin plates [3]. We have carried out a numerical experiment for plate models with different geometric configurations, thickness values, material parameters and mesh structure.

We have reached the following conclusions based on the results obtained:

1. Both implementations yielded close efficiency indices for all examples where fully clamped edges were given as boundary conditions; the error overestimation had a satisfactory value.

2. The distribution of the error indicator over the computational domain turned out to be almost identical for both implementations, which further confirms that they are correct.

It would be of interest to use this approach in adaptive solutions of applied problems with the help of the resources of the Polytechnic Supercomputer Center in the future.

M.E. Frolov's and O.I. Chistiakova's studies were carried out with the financial support of the grant of the President of the Russian Federation МД-1071.2017.1.

REFERENCES

[1] **R.S. Falk,** Finite elements for the Reissner – Mindlin plate, Mixed finite elements, compatibility conditions, and applications, Springer, Berlin, Heidelberg (2008) 195–232.

[2] **S.I. Repin, M.E. Frolov,** Estimation of deviations from the exact solution for the Reissner – Mindlin plate problem, Journal of Mathematical Sciences. 132 (3) (2006) 331–338.

[3] **M.E. Frolov,** Reliable a posteriori error control for solutions to problems of Reissner – Mindlin plates bending, Proceedings of 10th International Conference Mesh methods for boundary-value problems and applications, Kazan University Publishing House, Kazan, Russia (2014) 610–615.

[4] **M. Frolov, O. Chistiakova,** Adaptive algorithm based on functional-type a posteriori error estimate for Reissner-Mindlin plates // Advanced Finite Element Methods with Applications. Selected papers from the 30th Chemnitz Finite Element Symposium, Lecture Notes in Computational Science and Engineering (LNCSE). 128, Ch. 7 (2019).

[5] **P. Neittaanmäki, S. Repin,** Reliable methods for computer simulation: Error control and a posteriori estimates, Elsevier, Amsterdam, 2004.

[6] **S. Repin,** A posteriori estimates for partial differential equations, de Gruyter, Berlin, 2008.

[7] **O. Mali, P. Neittaanmдki, S. Repin,** Accuracy verification methods: Theory and algorithms, Springer Science+Business Media Dordrecht, 2014.

[8] **U. Langer, S. Repin, T. Samrowski,** A posteriori estimates for a coupled piezoelectric model, Russian Journal of Numerical Analysis and Mathematical Modelling. 32 (4) (2017) 259–266.

[9] **S. Repin, J. Valdman,** Error identities for variational problems with obstacles, ZAMM – Journal of Applied Mathematics and Mechanics. 98 (4) (2018) 635–658.

[10] **P.R. Bцsing, C. Carstensen,** Discontinuous Galerkin with weakly over-penalized techniques for Reissner – Mindlin plates, Journal of Scientific Computing. 64 (2) (2015) 401–424.

[11] **B. Kumar, M. Somireddy, A. Rajagopal,** Adaptive analysis of plates and laminates using natural neighbor Galerkin meshless method, Engineering with Computers. 35 (1) (2018) 201–214.

[12] **W. Dörfler,** A convergent adaptive algorithm for Poisson's equation, SIAM Journal on Numerical Analysis. 33 (3) (1996) 1106–1124.

[13] **R. Verfürth,** A review of a posteriori error estimation and adaptive mesh-refinement techniques. John Wiley & Sons, 1996.

[14] **A.S. Karavaev, S.P. Kopysov,** A refinement of unstructured quadrilateral and mixed meshes, Vestnik Udmurtskogo Universiteta. Matematika. Mekhanika. Komp'yuternye Nauki. (4) (2013) 62–78.

[15] **C. Carstensen, X. Xie, G. Yu, T. Zhou,** A priori and a posteriori analysis for a locking-free low order quadrilateral hybrid finite element for Reissner–Mindlin plates, Computer Methods in Applied Mechanics and Engineering. 200 (9–12) (2011) 1161–1175.

Received 29.12.2018, accepted 02.02.2019 .

THE AUTHORS

KISELEV Kirill V.
Peter the Great St. Petersburg Polytechnic University
29 Politechnicheskaya St., St. Petersburg, 195251, Russian Federation
kvladimirovich10@gmail.com

FROLOV Maxim E.
Peter the Great St. Petersburg Polytechnic University
29 Politechnicheskaya St., St. Petersburg, 195251, Russian Federation
frolov_me@spbstu.ru

CHISTIAKOVA Olga I.
Peter the Great St. Petersburg Polytechnic University
29 Politechnicheskaya St., St. Petersburg, 195251, Russian Federation
Chistiakova.Olga@gmail.com

СПИСОК ЛИТЕРАТУРЫ

1. **Falk R.S.** Finite elements for the Reissner – Mindlin plate // Mixed finite elements, compatibility conditions, and applications. D. Boffi, L. Gastaldi (Eds). Berlin, Heidelberg: Springer, 2008. Pp. 195–232.

2. **Репин С.И., Фролов М.Е.** Об оценке отклонений от точного решения задачи о пластине Рейсснера – Миндлина // Краевые задачи математической физики и смежные вопросы теории функций. Записки научных семинаров ПОМИ. СПб, 2004. Т. 310. С. 145–157.

3. **Фролов М.Е.** Надежный апостериорный контроль точности решений задач об изгибе пластин Рейсснера – Миндлина // Сеточные методы для краевых задач и приложения. Материалы Десятой международной конфеи ренции. Казань, 2014. С. 610–615.

4. **Frolov M., Chistiakova O.** Adaptive algorithm based on functional-type a posteriori error estimate for Reissner-Mindlin plates // Advanced Finite Element Methods with Applications. Selected papers from the 30th Chemnitz Finite Element Symposium, Lecture Notes in Computational Science and Engineering (LNCSE). 2019. Vol. 128. Ch. 7.

5. **Neittaanmдki P., Repin S.** Reliable methods

for computer simulation: Error control and a posteriori estimates. Amsterdam: Elsevier, 2004. 304 p.

6. **Repin S.** A posteriori estimates for partial differential equations. Berlin: de Gruyter, 2008. 316 p.

7. **Mali O., Neittaanmäki P., Repin S.** Accuracy verification methods: Theory and algorithms. Springer Science+Business Media Dordrecht, 2014. XIII+355 p.

8. **Langer U., Repin S., Samrowski T.** A posteriori estimates for a coupled piezoelectric model // Russian Journal of Numerical Analysis and Mathematical Modelling. 2017. Vol. 32. No. 4. Pp. 259–266.

9. **Repin S., Valdman J.** Error identities for variational problems with obstacles // ZAMM – Journal of Applied Mathematics and Mechanics. 2018. Vol. 98. No. 4. Pp. 635–658.

10. **Bösing P.R., Carstensen C.** Discontinuous Galerkin with weakly over-penalized techniques for Reissner – Mindlin plates // Journal of Scientific Computing. 2015. Vol. 64. No. 2. Pp. 401–424.

11. **Kumar B., Somireddy M., Rajagopal A.** Adaptive analysis of plates and laminates using natural neighbor Galerkin meshless method // Engineering with Computers. 2018. Vol. 35. No. 1. Pp. 201–214.

12. **Dörfler W.** A convergent adaptive algorithm for Poisson's equation // SIAM Journal on Numerical Analysis. 1996. Vol. 33. No. 3. Pp. 1106–1124.

13. **Verfürth R.** A review of a posteriori error estimation and adaptive mesh-refinement techniques. John Wiley & Sons, 1996. 127 p.

14. **Караваев А.С., Копысов С.П.** Перестроение неструктурированных четырехугольных и смешанных сеток // Вестник Удмуртского университета. Серия Математика. Механика. Компьютерные науки. 2013. Вып. 4. С. 62–78.

15. **Carstensen C., Xie X., Yu G., Zhou T.** A priori and a posteriori analysis for a locking-free low order quadrilateral hybrid finite element for Reissner –Mindlin plates // Computer Methods in Applied Mechanics and Engineering. 2011. Vol. 200. No. 9–12. Pp. 1161–1175.

Статья поступила в редакцию 29.12.2018, принята к публикации 02.02.2019.

СВЕДЕНИЯ ОБ АВТОРАХ

КИСЕЛЕВ Кирилл Владимирович – *магистрант кафедры прикладной математики Института прикладной математики и механики Санкт-Петербургского политехнического университета Петра Великого.*

195251, Российская Федерация, г. Санкт-Петербург, Политехническая ул., 29
kvladimirovich10@gmail.com

ФРОЛОВ Максим Евгеньевич – *доктор физико-математических наук, директор Института прикладной математики и механики, заведующий кафедрой прикладной математики Санкт-Петербургского политехнического университета Петра Великого.*

195251, Российская Федерация, г. Санкт-Петербург, Политехническая ул., 29
frolov_me@spbstu.ru

ЧИСТЯКОВА Ольга Игоревна – *аспирантка кафедры прикладной математики Института прикладной математики и механики Санкт-Петербургского политехнического университета Петра Великого.*

195251, Российская Федерация, г. Санкт-Петербург, Политехническая ул., 29
Chistiakova.Olga@gmail.com